RECENT WORK ON TIME-DOMAIN ANALYSIS

by

Allan Magee and Brad King

Continuing research at DCN BASSIN D'ESSAIS DES CARÈNES is being devoted to the development of a computer code which permits the solution of both the large-amplitude and linearized motions of a body of arbitrary shape. A time-domain approach is being used in which the linearized free surface condition allows the use of the Green function for an impulsive source to solve both problems.

To formulate the problem at hand, an ideal incompressible fluid is assumed. The fluid motion is irrotational and the velocity potential satisfies Laplace's equation. If $\vec{v}$ is the velocity vector of the fluid motion, then

$$\vec{v} = \vec{\nabla}\phi, \quad \Delta\phi = 0 \tag{1}$$

An inertial coordinate system is chosen with the z-axis upwards and the origin at the calm water level. The fluid domain is bounded by the free surface, the body surface, and a bounding surface at infinity. The linearized free surface boundary condition is :

$$[\phi_{tt} + g\,\phi_z]_{z=0} = 0 \tag{2}$$

On the body surface, the no-penetration condition is given by :

$$\phi_n = \vec{V}\cdot\vec{n} - \phi_{0n} \quad \text{on} \quad S_0(t) \tag{3}$$

where $\vec{n}$ is the the unit normal out of the fluid, $\vec{V}$ is the velocity of the body and ϕ_0 is the incident wave potential. This condition is applied on either the mean three-dimensional position of the body in the linear problem, or on the time-dependent three-dimensional moving surface in the large-amplitude problem. The motion starts smoothly from rest so that the initial conditions are :

$$\phi = 0, \quad \phi_t = 0 \quad \text{as} \quad t \to -\infty \tag{4}$$

Using the appropriate arguments in the far field, the desired integral equation for the velocity potential becomes :

$$\begin{aligned} 4\pi\,\phi(P,t) + \int_{S_0(t)} ds_Q\,\phi(Q,t)\,\frac{\partial G}{\partial n}(P,Q) &= \int_{S_0(t)} ds_Q\,G(P,Q)\,\frac{\partial \phi}{\partial n}(Q,t) \\ &- \int_{-\infty}^{t} d\tau \int_{S_0(\tau)} ds_Q \left[\phi(Q,\tau)\,\frac{\partial H}{\partial n}(P,Q,t-\tau) - H(P,Q,t-\tau)\,\frac{\partial \phi}{\partial n}(Q,\tau)\right] \end{aligned} \tag{5}$$

with

$$\begin{aligned} G(P,Q) &= \frac{1}{r_{PQ}} - \frac{1}{r'_{PQ}} \\ H(P,Q,t) &= 2\int_0^{\infty} d\kappa\,\sqrt{\kappa g}\,\sin(\sqrt{g\kappa}\,t)\,\exp(\kappa(z+\varsigma))\,J_0(\kappa R_{PQ}) \quad \text{for} \quad t \geq 0 \\ H(P,Q,t) &= 0 \quad \text{for} \quad t < 0 \end{aligned} \tag{6}$$

$$
\begin{aligned}
P &= (x,y,z), \quad Q = (\xi,\eta,\varsigma) \\
r_{PQ} &= \sqrt{(x-\xi)^2 + (y-\eta)^2 + (z-\varsigma)^2} \\
r'_{PQ} &= \sqrt{(x-\xi)^2 + (y-\eta)^2 + (z+\varsigma)^2} \\
R_{PQ} &= \sqrt{(x-\xi)^2 + (y-\eta)^2}
\end{aligned}
$$

and J_0 is the Bessel function of the first kind of order zero.

To solve the integral equation (5) the surface of the body is discretized into a number of triangular panels. The potential is assumed to vary linearly over each triangle :

$$\phi \simeq \sum_{\alpha=1}^{3} \phi_\alpha \, N_\alpha(s,t) \tag{7}$$

where s and t are the local cartesian coordinates situated on the panel, α is the index of the triangle corners, and the shape functions are given by :

$$N_\alpha(s,t) = a_\alpha + b_\alpha \, s + c_\alpha \, t \tag{8}$$

where a, b, and c are constants determined from the triangle geometry. The tangential derivatives of the potential are constant over each panel :

$$\frac{\partial \phi}{\partial s} \simeq \sum_{\alpha=1}^{3} \phi_\alpha \, b_\alpha, \quad \frac{\partial \phi}{\partial t} \simeq \sum_{\alpha=1}^{3} \phi_\alpha \, c_\alpha \tag{9}$$

Taking into account the contributions from the singular integrals, a known boundary condition is applied and (5) solved for the unknown values of the potential at points on the body. The solution proceeds by time stepping from rest. Once calculated, the potential and velocities are used in Bernoulli's equation to determine the pressure which is in turn integrated over the body to determine the generalized forces.

The numerical evaluation of the right hand side of the integral equation is performed by collocation not at the panel corners, but at the centroids. Since there are more panels than nodes, an over-determined system of equations results. This is solved by singular value decomposition, Numerical Recipes (1986), so the usual back-substitution step of LUD decomposition is replaced by simple matrix multiplication.

The method of Cantaloube and Rehbach (1986) is used to integrate $1/r$ and $1/r'$ and their normal derivatives over panels. The method uses Stokes theorem to convert the surface integrals over flat panels into line integrals around the panel edges. The required integrals (with different notation than the original) are given by :

$$\int_{S_e} ds_Q \, \frac{1}{r_{PQ}} = \vec{n} \cdot \int_C \frac{\vec{r}_{PQ} \times d\vec{\ell}_Q}{r_{PQ}} + \int_C \frac{(\vec{n}\cdot\vec{r}_{PQ})(\vec{e}\times\vec{r}_{PQ})\cdot d\vec{\ell}_Q}{r_{PQ}\,(r_{PQ} - \vec{e}\cdot\vec{r}_{PQ})} \tag{10}$$

$$
\begin{aligned}
\int_{S_e} ds_Q \, \mu \, \frac{\partial}{\partial n}\left(\frac{1}{r_{PQ}}\right) &= -\int_C \frac{\mu\,(\vec{e}\times\vec{r}_{PQ})\cdot d\vec{\ell}_Q}{r_{PQ}\,(r_{PQ} - \vec{e}\cdot\vec{r}_{PQ})} \\
&\quad - (\vec{e}\cdot\vec{n})(\vec{n}\times\vec{\nabla}\mu) \cdot \int_C \ln(r_{PQ} - \vec{e}\cdot\vec{r}_{PQ}) \, d\vec{\ell}_Q
\end{aligned} \tag{11}
$$

where,

$$\vec{e} = \pm\vec{n} \tag{12}$$

The sign of $\vec{e}$ is in general arbitrary, but one should have $\vec{e} = \vec{n}$ when $\vec{r}_{PQ}$ is in the plane of the panel and it is preferable to avoid the situation where $r_{PQ} - \vec{e} \cdot \vec{r}_{PQ}$ becomes too small. Given an appropriate choice of $\vec{e}$ the integrands are not singular unless the field point P is on the countour, which is never the case here. The line integrals are computed using a standard Gauss quadrature rule with different numbers of integration points for large and small separation of source segment and field points.

The integrals of the wave terms over the panels are approximated by a one-point Gauss rule between panel centroids.

To date, results are available for the linear radiation and exciting force coefficients at zero forward speed on a submerged ellipsoid, a floating hemisphere, and a Wigley seakeeping hull. Figure 1 shows the computed real and imaginary parts of the surge exciting force on a submerged ellipsoid in head waves versus nondimensional wave number compared with numerical computations performed with the frequency domain computer code DIODORE using the same geometric discretization. The number of trianglar elements was 132 on one fourth of the body. For the present method, the frequency-domain representation was obtained by taking the Fourier transform of the time-domain record, obtained as the response to a nonimpulsive input. Also shown in the figure are the analytic results of Wu and Eatock-Taylor (1987).

Figure 2 presents the nondimensional heave added mass and damping coefficeints versus nondimensional frequency computed by the present method for the Wigley hull at zero forward speed. Comparisons with other numerical calculations are forthcoming.

The velocity potential for the semi-infinite fluid problem corresponding to the infinite frequency limit ($\phi = 0$) of the frequency-domain free surface condition for the pitching Wigley hull is shown in figure 3.

Unsteady forces due to the large amplitude forced motions of a submerged sphere are presented in figure 4 for one case of motion amplitude and frequency, along with the steady-state results of Ferrant (1989). There are slight differences in the predicted steady-state force. This may be due to the differences in problem formulation (source distribution as opposed to the present Green's theorem formulation), due to the different finite differencing schemes used to calculate the time-derivative of the potential, or due to the finite resolution of the time and space discretizations used in the respective calculations.

The coupling between the dynamic equation of motion and the hydrodynamic forces is presently the object of further study. Modules have been written and their proper functioning is being assured. Updated results will be presented at the workshop.

This work is the result of research supported partly by DGA/DRET, under contract number 89/1051. This support is gratefully acknowledged.

References

[1] Cantaloube, B., and C. Rehbach. 1986. Calcul des intégrales de la méthode des singularités. *La Recherche Aerospatiale,* 1: 15-22.

[2] Ferrant, P. 1989. Radiation d'ondes de gravité par les mouvements de grande amplitude d'un corps immergé : Comparaison des approaches fréquentielle et instationaire. Ph.D. Diss., ENSM, Nantes.

[3] Press, W. H., *et al.*, 1986. *Numerical Recipes.* Cambridge, UK: Cambridge University Press.

[4] Wu, G. X., and R. Eatock-Taylor. 1987. The exciting force on a submerged spheroid in regular waves. *Journal of Fluid Mechanics,* (182): 411–426.

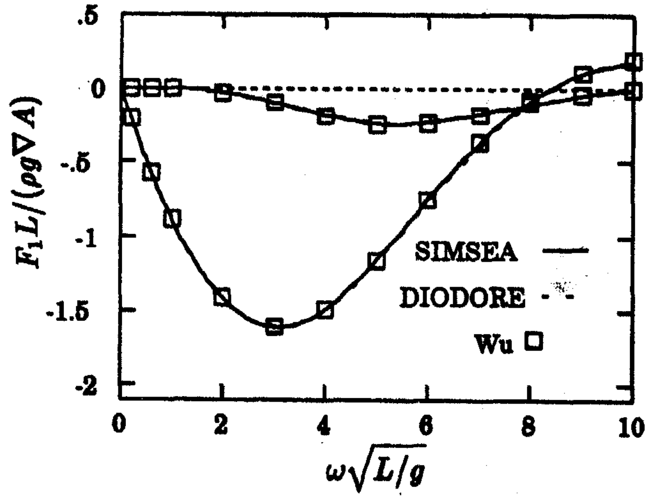

Fig.1. **Real and imaginary parts of the surge exciting force for a submerged ellipsoid.**

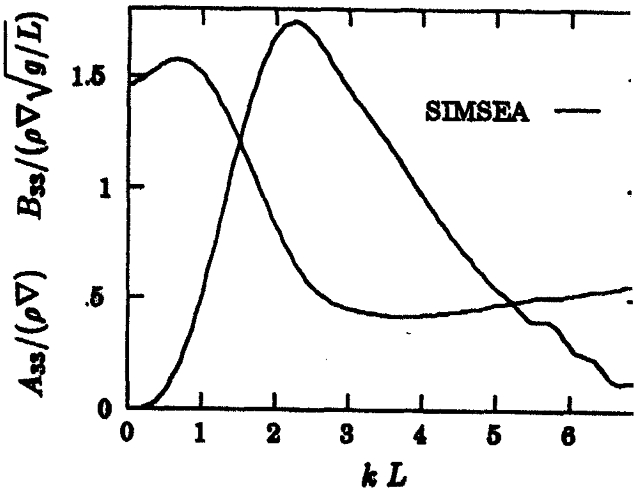

Fig.2. **Heave added mass and dampi[ng] for a Wigley hull.**

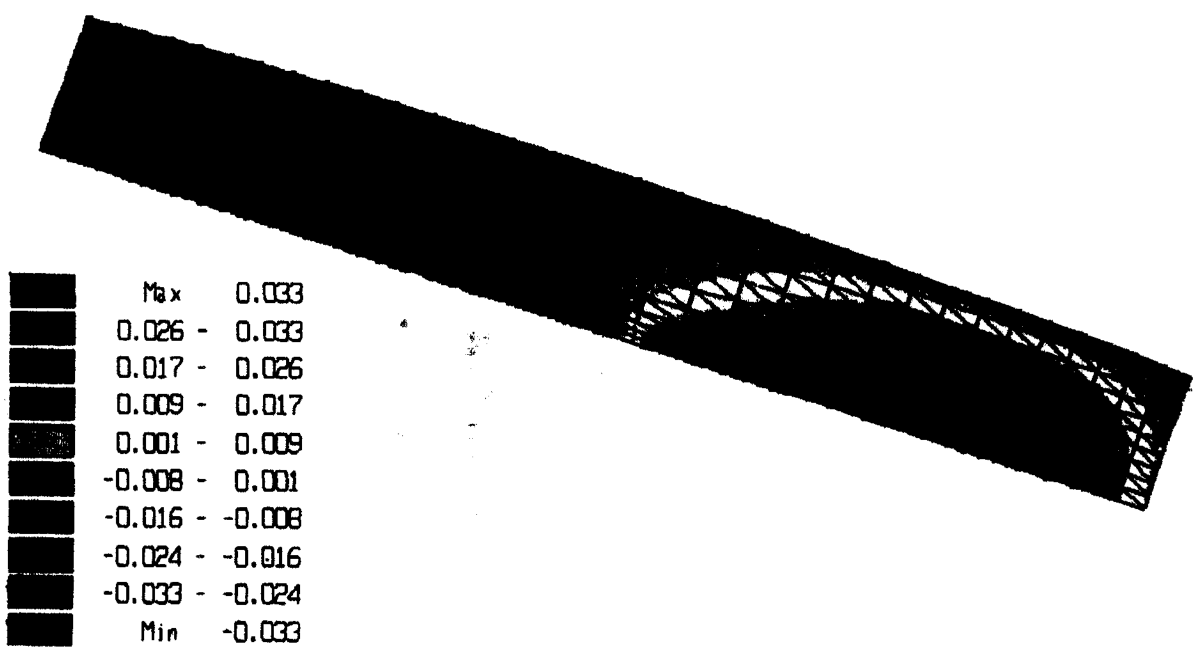

Fig.3. **Velocity potential on a pitching Wigley hull using a ($\phi = 0$) free surface condition.**

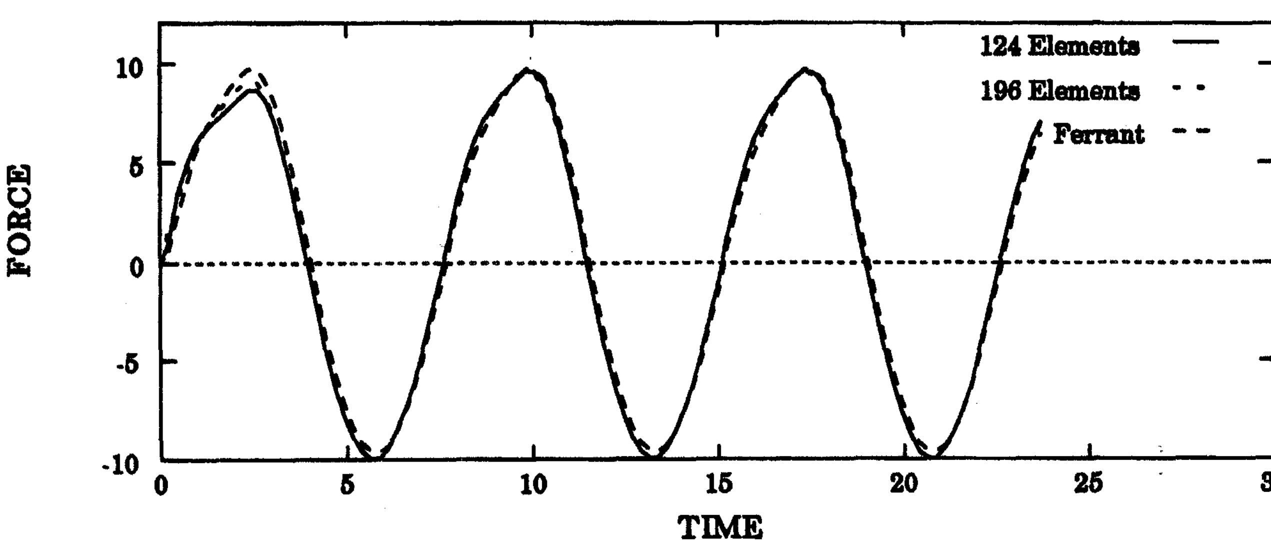

Fig.4. **Force on a submerged heaving sphere in large amplitude motion.**

DISCUSSION

GREENHOW: To be consistent with the linear free surface condition, the ***finite*** body amplitude method should then only be applied to slow motions. It would then be interesting to look at the motions of submerged cylinders and spheres very close to the free surface, where there is a strong variation in added mass. I have recently done same exact nonlinear calculations fot the former case — Let's compare the two methods!

MAGEE & KING: We agree that there are restrictions on the application of the finite-amplitude formulation which retains the linearized free surface condition, namely, that the waves be of small slope. It would be interesting to compare fully linear, finite-amplitude, and fully nonlinear calculations to determine the limits of applicability (validity) of each one, and the relative importance of the finite-amplitude and nonlinear free surface effects.

MARTIN: Is there any particular virtue in using triangular panels rather than quadrilateral panels?

MAGEE & KING: There are several advantages in using triangular instead of quadrilateral panels, for instance:

• The well-known fact that there are no gaps between triangle edges, and that the vertices lie exactly on the body surface. The potentially dangerous situation where a quadrilateral panel edge may slightly pierce the free surface or cross the symmetry plane is thus avoided.

• It is easier to program the generation of triangles — no least-squares fitting is required as in the case of Hess and Smith type quadrilaterals. Note also the current trend in CFD towards using unstructured triangular meshes to discretize complex geometrical configurations, evidently because automatic algorithms are readily available for this task.

• With the present method satisfying the boundary conditions at the panel centroids for the unknowns at the nodes, it is necessary to use at least some triangles (for a rectangular mesh) to make the number of equations greater than or equal to the number of unknowns in order that the system is solvable.

• Interfacing with CAD and finite element codes using pointwise representation of a surface is easier. Given such a representation, we need only an element connectivity algorithm to 'connect the dots', preserving the original surface in the hydrodynamic calculation.

It is not clear whether the numerical error is reduced using an equivalent number of triangles instead of quadrilaterals. At times one or the other appears better. For discretizations of realistic hull shapes, it is often convenient to apply triangles near the ends and quadrilaterals in the parallel middle body. The ideal method should have the capability of using either or both.

LIN: The numerical examples you shown for Wigley Hull and Sphere use "structured" triangular grid. Theoretically, unstructured triangular mesh which concentrate panels in areas where velocity or potential vary fast can be used to improve solution accuracy. Is it feasible to use unstructured panel for this problem,

DISCUSSION

will it cause any problem in numerical calculation especially in velocity evaluation which requires spatial differentiations in potential formulation.
MAGEE & KING: In fact, the triangular panels were chosen with this in mind. Element connectivity is included for unstructured grids. The linear variation was chosen so that spatial first derivatives are very easy to calculate.

NEWMAN: For flat triangular panels and linear distributions you could evaluate the Rankine influence function analytically in the near field, and from multipole expansions in the far field. Why do you use Gauss quadratures instead?
MAGEE & KING: The required analytic formulas are more complicated than the present numerical scheme. By avoiding ATAN functions, we hope to improve the speed of the calculation. Initial calculations using the formulas of Webster and Yeung did indeed show this, but perhaps further investigation is needed in the light of the discussion by Noblesse (see below).
The use of multipole expansions may require more 'IF' statements, thus further slowing calculations. Alternatively, one can put all the 'IF' statements in one loop, and pass a vector of arguments to separate subroutines or loops, one for each expansion, thus separating the bulk of the calculations into vectorizable loops. This increases the overhead, but may speed up the calculation, depending on the type of machine being used. The present method is being applied on an Alliant FX/80 parallel-vector architecture.
We note also that the present scheme is stable as the field point approaches the plane of the panel.

NOBLESSE: Based on our experience, it is efficient to use Gauss integration rules for evaluating the potential of source and dipole distributions over flat panels, except in the immediate vicinity of the panels where we use exact analytical formulae. Gauss rules can also be more accurate: for instance, the one-point rule becomes more accurate, using single precision calculation, than the analytical formulae at a distance from the panel equal to about 10 times the longest side of the panel.